ORIGINAL PAPER

Preparation of novel arsenic-imprinted polymer for the selective extraction and enhanced adsorption of toxic As^{3+} ions from the aqueous environment

Muhammad Saqaf Jagirani[1] · Aamna Balouch[1] · Sarfaraz Ahmed Mahesar[1] · Ameet Kumar[1] · Abdullah[1] · Faraz Ahmed Mustafai[1] · Muhammad Iqbal Bhanger[2]

Abstract

In this study, we prepare synthetic arsenic-imprinted polymer (As-IP) by simple precipitation polymerization method by using 4-vinyl pyridine and 2-hydroxyethyl methacrylate as ligand and functional monomer use for the selective elimination of arsenic (As^{3+}) from the aqueous environment. To achieve maximum sorption capacity several factors, i.e., pH, agitation time, shaking speed and sorbent dose were optimized. This prepared polymer was characterized by using SEM, EDX and FT-IR. Adsorption isotherm and kinetic data of As^{3+} follow the Langmuir isotherm and pseudo-second-order kinetic model. The maximum sorption capacity of As-IP is 106.3 mg/g. The limit of detection and limit of quantification were found to be 0.87 and 2.9 µg/L, respectivley. The relative selectivity factors of As-IP as compared to NIP for As^{3+}/Cr^{3+}, As^{3+}/Al^{3+}, As^{3+}/Ni^{2+}, As^{3+}/Cu^{2+}, As^{3+}/NO$_3^-$, As^{3+}/PO$_4^{3-}$ and As^{3+}/SO$_4^{2-}$ were 1.445, 1.779, 1.469, 1.168, 1.481, 1.802 and 2.367, respectively. The adsorption efficiency of As^{3+} ions by using As-IP from real water samples was approximately 99% which shows that As-IP has good sorption capability and highly selective for the extraction of arsenic ions.
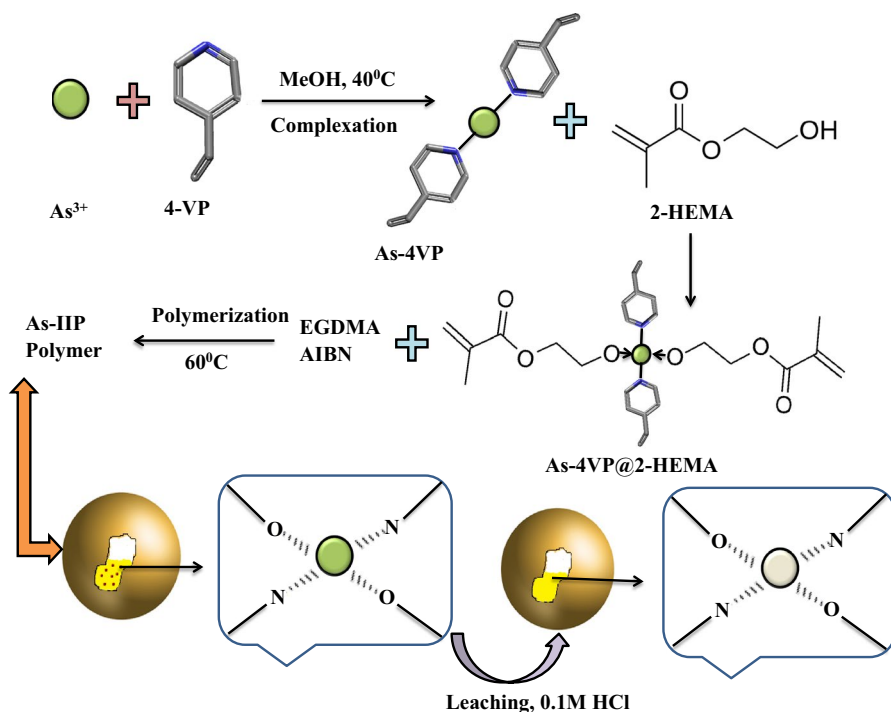
✉ Aamna Balouch
aamna_balouch@yahoo.com

1   National Centre of Excellence in Analytical Chemistry, University of Sindh, Jamshoro, Pakistan

2   HEJ Research Institute of Chemistry, International Center for Chemical Sciences and Biological Sciences, University of Karachi, Karachi, Pakistan

Graphic abstract

Graphical representation of As-IP

Introduction

Arsenic (As) is known as a highly toxic pollutant that seriously threatens the environment and human health [1, 2]. Especially, As^{3+} is highly toxic than As^{5+}. Uptake of the very low amount of As^{3+} compounds can be fatal [3, 4]. The major causes of As toxicity are mining, fossil fuel combustion, biogeochemical reactions, pesticides and other As-based additives, although mostly population exposed to As via food, soil, air, and water. Drinking water has significant influences on human health. The As concentration fluctuates on the nature of water (groundwater, lake water, surface water) [5, 6]. As^{3+} is considered as a carcinogenic element and has adverse effects on human health and causes skin diseases, lungs diseases, prostate cancer and nasal passage [7–9]. The permissible limit is given by the world health organization (WHO) for As in drinking water is 0.010 mg/L [2]. Countless methods are reported for the treatment of As from aqueous system, i.e., chemical precipitation, coagulation, oxidation, membrane filtration, ion exchange and adsorption [10–16]. The

process of adsorption which used different kinds of sorbents for the detoxification of toxic heavy metals from wastewater due to its efficiency and simplicity, i.e., bio-sorbents, activated carbon, chitosan, industrial waste sorbents and chelating resins [2, 9, 17–21], etc. However, various studies also indicate that these above-mentioned adsorbents can extract As^{3+} but they are not much selective. To highlight these problems, researcher desired to prepare low-cost and an environment-friendly adsorbent which retains higher adsorption capacity and selectivity. Ion-imprinted polymers (IIPs) have an unrivaled advantage for selective extraction and recapture of toxic metal ions due to their selective binding cavities which are complementary to that target analyte [22–24]. Thus, IIPs are known to be the new area of selective sorbents which can also be chemically regenerated and reusable, which further decreased the treatment cost [25, 26]. In an IIPs method, the selectivity of polymeric material depends upon the definite behavior of functional monomer and ligand, on the coordination geometry and coordination number of heavy metal ions as well as their sizes and charges [27–29]. IIPs have an important role in the selective removal of toxic heavy metal ions from the wastewater [30]. Different methods, i.e., suspension polymerization, precipitation polymerization, surface imprinting polymerization and bulk polymerization are used for the development of IIPs [31, 32]. Several types of IIPs have been synthesized and used selective detoxification of heavy metals, i.e. Pb, Cu, Cd, Ni and Hg. Fang et al. [2] synthesized arsenite IIPs with tetra, bromine-bi-4, 5-2(methylene, bi-imidazole) as a functional monomer which shows good adsorption capacity toward target analyte. Zhou et al. [33] prepared Ni^{2+}-IPs for removal of Ni^{2+} ions from wastewater. The maximum sorption capability was 86.3 mg/g, at pH 7.0. Faraz et al. prepared imprinted material for the selective elimination of As ion from aqueous media [6]. The adsorption capacity was reported 0.175 mg/g at pH 7.0.

In this study, As-IP was synthesized by using co-precipitation, polymerization method with 4-vinyl pyridine (4-VP), 2-(hydroxyethyl) methacrylate (2-HEMA) as a ligand and functional monomer, ethylene glycol methacrylate (EGDMA) as a crosslinker and 2,2-azobisisobutyronitrile (AIBN) as an initiator for the selective detoxification of As^{3+} from the aqueous environment. The synthesized polymer was characterized by FT-IR, EDX and SEM, and the effect of sorption conditions such as pH, temperature, contact time, shaking speed and sorbent dose was also optimized. The selectivity studies of As-IP were also studied by choosing Ni^{2+}, Co^{2+}, Cr^{3+}, Cu^{2+}, NO_3^-, SO_4^{2-} and PO_4^{3-} as coexisting ions and used in real aqueous samples.

Materials and methods

Reagents

Sodium arsenite (Na_2AsO_3) and copper sulfate pentahydrate ($CuSO_4.5H_2O$) were obtained from Merck (Germany). 2,2-Azobisisobutyronitrile (AIBN), nickel chloride hexahydrate ($NiCl_2 \cdot 6H_2O$), hydrochloric acid (HCl) chromium chloride hexahydrate ($CrCl_3 \cdot 6H_2O$) were purchased from Dae-Jung Chemicals (South Korea). 2-(Hydroxyethyl), methacrylate, (2-HEMA) and ethylene glycol dimethacrylate

(EGDMA) were purchased from Alfa Aesar (England), varamine blue was purchased from (BDH, UK), 4-vinylpyridine(4-VP) and methanol were obtained from Sigma-Aldrich (USA), and ELGA ultrapure Milli-Q water (USA) used all over the experiment. All the above chemicals were analytical grade and used without further purifications.

Real water sample

To check the applicability of synthesized imprinted polymer, the real aqueous samples were collected from the channel canal near Hyderabad, Sindh, Pakistan. The samples were collected in fresh plastic bottles and rinsed with distilled water. The collected water samples were filtered by 0.45-μm pore size membrane to remove the colloidal particles. Then all samples were properly labeled and stored at about 4 °C prior to analysis.

Synthesis of As³⁺-imprinted polymer

As-IP was prepared by using co-precipitation polymerization method. The IIP was prepared by adopting the protocol from Onnby et al. [34] and Fang et al. [2]. To prepare IIP for As, first 1-mmol of Na_2AsO_3 salt as a template and 2-mmol of 4-vinyl pyridine (4-VP) as a ligand were completely dissolved in the 50 mL of methanol as a solvent in 100-mL sealed round-bottom flask and allowed 20 min to form a complex. After 20 min, 8 mmol of 2-hydroxy methacrylate (2-HEMA) was added and stirred up to 30 min to form As^{3+}/4-VP/2-HEMA complex, respectively. After the complex formation, 20 mmol of ethylene glycol dimethacrylate (EGDMA) was added as a crosslinker and 0.1 g of 2,2′-azobisisobutyronitrile (AIBN) was added as an initiator to initiate the reaction and form the radicals, and then the solution was stirred for 30 min at room temperature. Finally, the solution was degassed with inert nitrogen gas for 20 min to remove the dissolved oxygen from the reaction mixture. The flask was tightly sealed with parafilm and started the polymerization reaction at 60 °C for 12 h. After the polymerization, the resultant polymer product was washed with 1:4 v/v of water and methanol to eliminate the unreacted substances from the polymer matrix, and the resulting IIP was leached with 0.1 M HCl to leach the As^{3+} ions from the polymer matrix and form the selective recognition binding sites and then washed the polymer with Milli-Q water until a neutral pH was achieved. The resulting polymer product was dried at 55 °C for the sorption studies. Non-imprinted polymers (NIPs) were prepared using the same method without the template.

Characterization

The characterization of As^{3+}-IP and NIP was carried out by using the Fourier transform infrared spectroscopy (FT-IR), energy-dispersive X-ray (EDX), and scanning electron microscope (SEM), and the FT-IR (Thermo Nicolet 5700) was used to check the functionality of As^{3+} IPs and NIPs. SEM was used to check the surface morphology of the IIPs and NIPs and leached IIPs by using (JSM, 6380 of

Joel, Japan) operating at 20 kV. The pore volume and surface area were analyzed by Brunauer–Emmett–Teller (BET) (Quantachrome® ASiQwin™ V.5, USA). The elemental arrangement of As-IP, NIPs and leached IIPs was investigated by X-ray (EDX), and analyzer was furnished with a scanning electron microscope.

Adsorption method

The sorption efficiency of As^{3+} ion was checked by the batch adsorption method from the aqueous media. The As^{3+}-IPs were added into 10 mL solution of As^{3+} ions concentration that ranges from 5 to 25 mg/L. The 0.1 M solution of NaOH and HCl was used for adjusting the pH from 2 to 10. The adsorption take place by shaking the solution for 15 min at 50 °C after that the solution was filtered, and the elute was analyzed on UV/Vis spectrometer. The sorption capability of the As^{3+}-IPs was calculated by using the following formula.

$$Q = \frac{C_o - C_f}{w} * V$$

where Q represents the sorption capacity of IP (mg/g), C_o and C_f are the existing and ultimate concentration of the As^{3+} ions (mg/L) in the solution, V represents the volume of the solution (L) and (w) shows the weight of IIPs added in the solution (g).

The selectivity of As^{3+}-IP was also conducted by batch adsorption method. 0.1 g of As^{3+}-IP was added in 10 mL of solution which contains 10 mg/L of As^{3+}/Cr^{3+}, As^{3+}/Al^{3+}, As^{3+}/Ni^{2+}, As^{3+}/Cu^{2+}, As^{3+}/NO_3^-, As^{3+}/PO_4^{3-} and As^{3+}/SO_4^{2-} and stirred during sorption at pH 6.0 and temperature 40 °C. The distribution ratio (K_d), selectivity coefficient (K) and relative selective coefficient (K') values were calculated by using these equations

$$K_d = \frac{C_o - C_f}{C_o} * \left(\frac{V}{w}\right)$$

$$K = \frac{K_d(As^{3+})}{K_d(M_{int:})}$$

$$K' = \frac{K_{(imprinted)}}{K_{(non-imprinted)}}$$

where K_d, K and K show the distribution ratio, selectivity coefficient and relative selectivity coefficient, and M_{int} represents the other selected competitive metal ion.

Water sample analysis

To check the pH of water sample, the digital pH meter (Metrohm 781), was used. To determine the concentration of As^{3+} from the solution UV–visible spectrophotometer (Biochrom Libra S22) was used during analysis, whereas, the varamine blue was used as a complexing agent λ_{max} at 556 nm. Atomic absorption

spectrometer (AAS) (Perkin Elmer, Model Analyst 700, Norwalk, CT) was used for the quantification of metals, and ion chromatography (IC) was used to quantifying the anions from the solution (Metrohm, 861 Advanced Compact IC).

Results and discussion

Characterization

SEM analysis

The surface morphological analysis of NIP, As^{3+}-IPs and leached IPs (L-IP) was characterized by the low- and high-resolution SEM as shown in Fig. 1a–c. The SEM images showed that morphology of polymers was not significantly different from each other at low resolution images. Figure 1a exhibited some slight visible changes of NIP and As^{3+}-IP. The high resolution Fig. 1a shows that the surface of NIP seems less rough as compared to the surface of As-imprinted polymer. In Fig. 1a, the polymer particles were closely packed with each other; however, in Fig. 1b the particles were irregular, porous and fractured due to the successful imprinted of As^{3+} ions in the polymeric matrix. It could be noticed in Fig. 1c that after the elimination of As^{3+} ions from the IIPs the irregularity of polymer surface was increased. The increase in irregularity may be due to the elimination of As^{3+} ions from a polymer which forms selective recognition cavities inside the network.
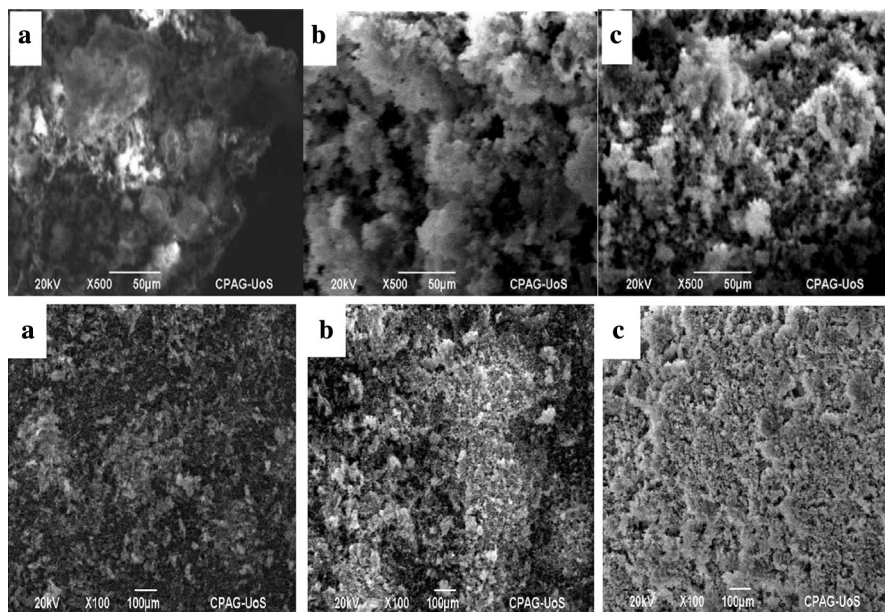

Fig. 1 Low- and high-resolution SEM images of NIP (**a**), As^{3+}-IP (**b**) and leached-IP (**c**)

Table 1 BET analysis of As^{3+}-IPs, L-IPs and NIPs

Polymer	Surface area (m^2/g)	Pore volume (cm^3/g)	Average pore diameter (Å)
As^{+3}-IPs adsorption	6.872	0.039	28.121
As^{+3}-IPs desorption	4.875	0.032	21.514
L-IPs adsorption	16.472	0.045	19.149
L-IPs desorption	5.450	0.028	21.528
NIPs adsorption	0.007	0.000	61.706
NIPs desorption	0.016	0.000	32.789
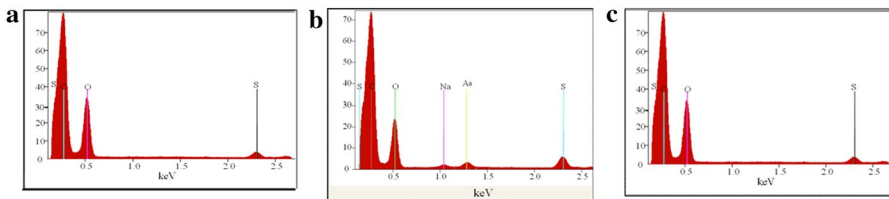
Fig. 2 EDX images of NIP (**a**), As^{3+}-IP (**b**) and leached-IIP (**c**)

BET analysis

The pore volume and surface area of the As^{+3} IPs and NIPs samples were analyzed by the automated gas sorption analyzer Brunauer–Emmett–Teller (BET). Around 80 mg of the dry polymers were degassed at 150 °C under the flow of nitrogen for approximately 4 h prior to analysis. The nitrogen adsorption/desorption data were recorded at (77°K) temperature using the liquid nitrogen. The pore volume and specific surface area were calculated by using BET equation. The micro-pores size distribution was determined by the Barrett–Joyner–Halenda (BJH) method. The results are shown in Table 1.

EDX analysis

EDX was used to check the elemental arrangement in NIPs, As^{3+}-IPs and L-IPs. Figure 2a shows the EDX spectrum of NIPs, where three peaks appeared of C, O, and S. It exhibits that synthesized polymer has no contamination. Figure 2b shows an extra peak of As^{3+} ion in the polymer matrix along with Na$^+$ ions, which evidenced the successful imprinting of As^{3+} ions in the polymeric matrix. However, the As^{3+} ions were leached from the resultant polymeric network in order to obtain highly selective recognition binding sites into a polymer network of corresponding size and shape. Figure 2c showed the absence of As^{3+} ions peak that confirmed the As^{3+} was successfully eliminated from the IIPs.

FT-IR analysis

FT-IR spectrum depicted in Fig. 3 shows the bending and stretching vibration of As^{3+}-IP and NIP. Both (As^{3+}-IP and NIP) spectra showed similar backbone and same stretching and vibration bands. The band at 3496.52 cm^{-1} indicate the stretching vibration band of OH group present in EGDMA. The band at 2995.49 cm^{-1} and 1728.27 cm^{-1} indicate the stretching band of C=O and C–H which was present in 2-HEMA and EGDMA. The band at 1466.03 cm^{-1} and 1163.90 cm^{-1} indicate the stretching band of C–N present in 4-vinyl pyridine group and C=C group which is also present in 2-HEMA and EGDMA. One additional peak at 471.26 cm^{-1} in As^{3+}-IP spectra was due to the introduction of As^{3+} ion in the polymeric network. Slight shifting of the band in As-IP was also observed due to the introduction of metal in the polymer.

Optimization studies

In order to achieve maximum sorption efficacy, various parameters were optimized, i.e., pH, time, shaking speed and sorbent dose.

Effect of pH

pH is an essential parameter in the sorption study, and it impacts the adsorption of toxic metal ions from the aqueous media. The effect of pH on the adsorption of Ar^{3+} ions on the polymeric surface was studied from 2 to 10. It was observed that the sorption efficiency of Ar^{3+} ions was raised from 2 to 6 on polymer surfaces and then moderately decreased as shown in Fig. 4. At acidic pH, the sorption efficiency was lower due to an excessive number of H^+ ions which interfere with the
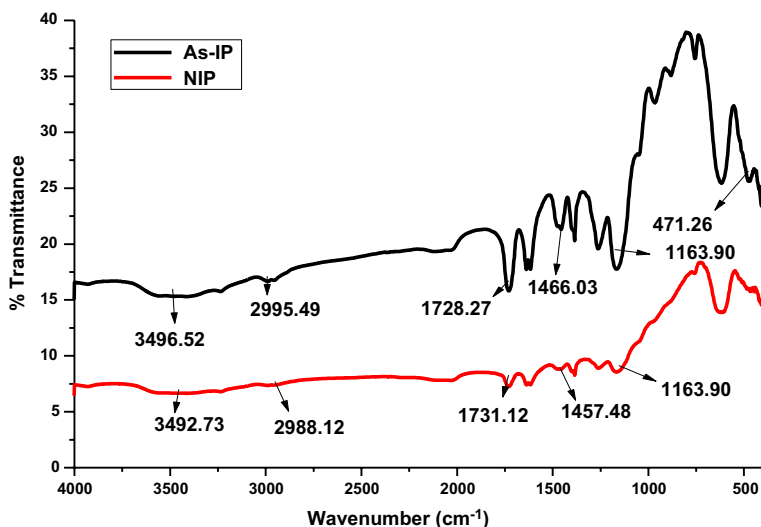

Fig. 3 FT-IR spectra of NIP (Red) and As-IP (Black) (colour figure onlinle)
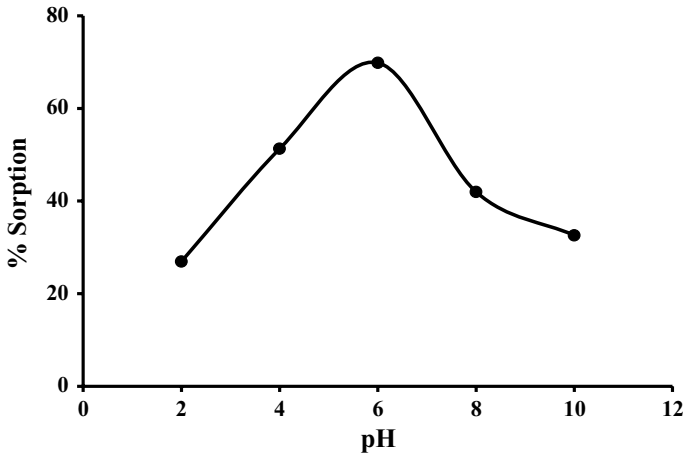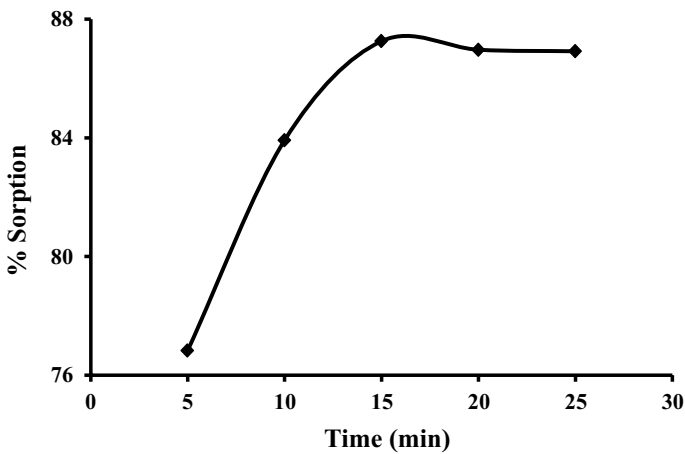
Fig. 4 Effect of pH on the sorption of Ar^{3+} ions

Fig. 5 Agitation time effect on the sorption capacity of As^{3+} ions

coordination of Ar^{3+} ions with functional monomer. At high basic pH, the sorption efficiency was reduced due to the precipitation of Ar^{3+} ions with OH^- ions so the pH 6.0 was optimized for other studies.

Effect of agitation time

The agitation time effect was checked from 5 to 25 min to obtain the maximum sorption efficacy, and other parameters were kept constant. It was observed that the maximum sorption achieved at 15 min as shown in Fig. 5. After 15 min, no
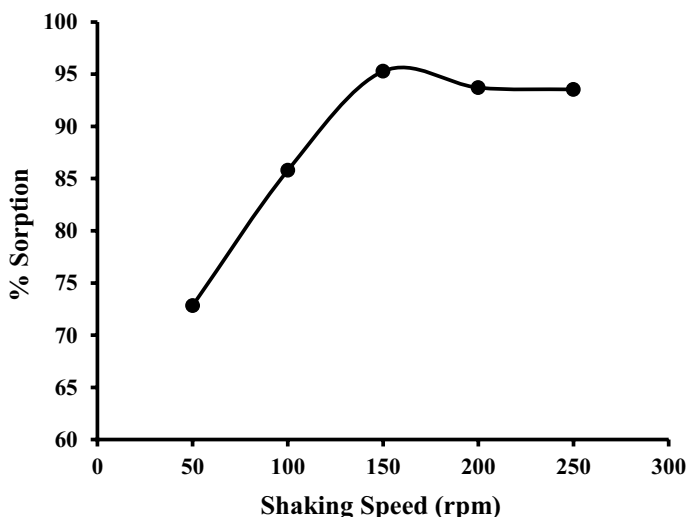
Fig. 6 Effect of shaking speed on the sorption of As^{3+} ions

significant changes were found in sorption uptake. Therefore, 15 min time was optimized for other studies.

Effect of shaking speed

The shaking speed effect was also checked to achieve the maximum adsorption efficacy from the range of 50–250 rpm. The batch sorption method was used to check out the effect of shaking speed and keep other parameters constant as shown in Fig. 6. The result shows that the sorption capability was increased with increasing the speed of shaking and found maximum sorption ability at 150 rpm, after that the sorption was decreased. The decrease in sorption was due to its high kinetic energy which decreased the interaction of sorbent and the initial concentration of the metal ion. Therefore, 150 rpm was optimized for further studies.

Effect of adsorbent dose

The sorbent dose was also optimized in order to gain maximum efficacy. The amount of sorbent dose in sorption studies increased in the range of 20–140 mg at the same metal ion concentration in the solution as shown in Fig. 7. The results indicated that, as the sorbent amount increased the percentage of adsorption also increased and found maximum sorption at 100 mg. There was no significant change in the sorption process noticed above 100 mg. Therefore, the 100 mg of the adsorbent dose was optimized for further studies.
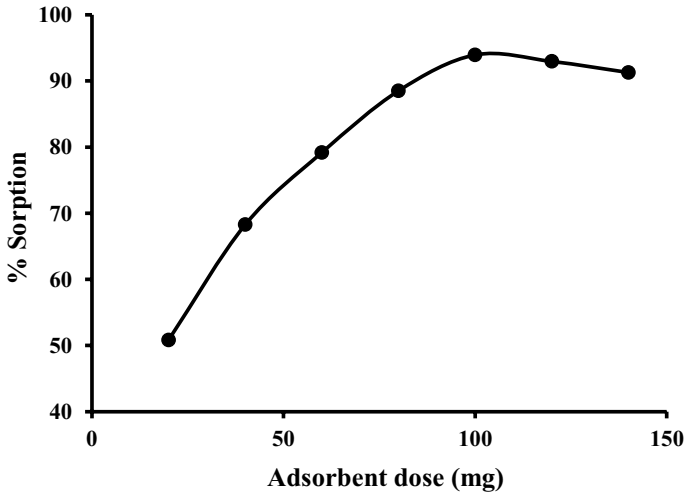
Fig. 7 Effect of adsorbent dose for the adsorption of As^{3+} ions

Adsorption isotherm

The elimination of As^{3+} was investigated by changing the concentration in the range of 5–25 mg/L by using 100 mg of adsorbent under optimized conditions. Langmuir and Freundlich's isotherm were used to study the sorption mechanism.

The Langmuir isotherm model According to the Langmuir isotherm model, the selective cavities on the surface of the polymer are homogenous and sorbate adsorb in the form of a monolayer. The Langmuir isotherm equation can be expressed as

$$\frac{C_e}{q_e} = \frac{1}{q_{max}b} + \frac{C_e}{q_{max}}$$

where C_e represents the equilibrium metal ion concentration in the equilibrium phase, mg/L; q_e is the sorption capability of metal ions on the polymeric matrix in mg/g; q_{max} indicates the maximum sorption capacity and b represents the Langmuir constant.

The Langmuir isotherm was checked out in the linear form. Figure 8a shows that the graph was plotted between C_e/C_{ads} and C_e which gives a traditional line. The Langmuir parameters were investigated by using slope, and intercept of linear graphs is displayed in Table 2. The values of R_L were observed in the range of 0.064–0.256.

The Freundlich isotherm model Freundlich isotherm model also was applied to check the multilayer form of adsorption of adsorbate on the surface of the polymer. The equation of Freundlich can be expressed as
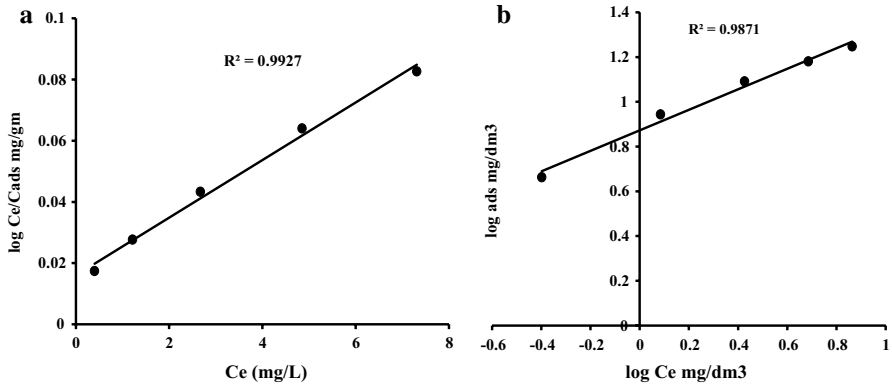
Fig. 8 Langmuir model (**a**) and Freundlich model (**b**) for the sorption of As^{3+} ions

Table 2 Langmuir and Freundlich isotherm constants for the sorption of As^{3+} ions

Langmuir				Freundlich			
q_0 (mg/g)	b (L/mg)	RL	R^2	n	$1/n$	K_f	R^2
106.3	0.58	0.064–0.256	0.992	2.177	0.459	7.454	0.987

$$\log q_e = \log k_f + \left(\frac{1}{n}\right) \log C_e$$

where n and K_f are shown as the Freundlich constants. The sorption method will be favorable if the value of $1/n$ will be in the array of 0–1.

It is decided that our experimental results are well followed toward the Langmuir isotherm as associated with the Freundlich isotherm based on the correlation coefficient and sorption capability of As-IP. The R^2 value of Langmuir isotherm was 0.992, whereas the R^2 value of Freundlich isotherm was 0.987 as shown in Fig. 8b, and isotherm constants value is given in Table 2. The Langmuir sorption capability of As-IP was 106.3 mg/g whereas the Freundlich sorption capacity was 7.454 mg/g, respectively.

Kinetics studies

The time attain to equilibrium is important for estimating the sorption efficiency of the polymer. To evaluate the equilibrium time of the sorption process, kinetics models such as pseudo-first order and pseudo-second order were applied in acquired experimental results. The pseudo-first order is represented in a given equation.
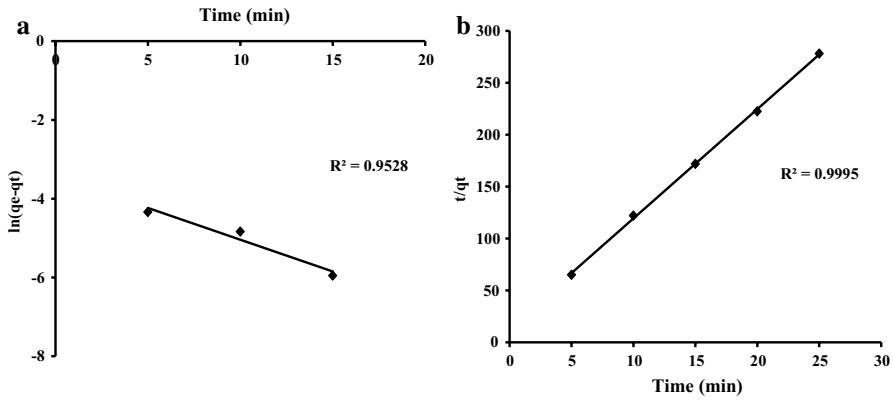
Fig. 9 **a** Pseudo-first-order and **b** pseudo-second-order model for the adsorption of As^{3+} ion

Table 3 Kinetic sorption model for the adsorption of As^{3+} ions

Pseudo-first order			Pseudo-second order		
K_1 (min^{-1})	q_e (mg/g)	R^2	K_2 (mg^{-1} min^{-1})	q_e (mg/g)	R^2
0.371	1.232	0.952	7.963	0.094	0.999

$$\log \left(q_e - q_t\right) = \log q_e - k_1 \frac{t}{2.303}$$

where q_e and q_t represent the sorption capabilities at the time (t) and at equilibrium time, and k_1 shows the sorption rate constant.

The equation represents the pseudo-second order

$$\frac{t}{q_t} = \frac{1}{k_2 q_e^2} + \frac{t}{q_e}$$

where q_t is the sorption capacity at the time (t), mg/g and k_2 show the rate constant.

It was observed that our experimental results are well followed toward the pseudo-second order based on R^2 value. The value of R^2 in pseudo-second order is 0.999, while the R^2 value in pseudo-first order is 0.952 as shown in Fig. 9 and Table 3

Adsorption thermodynamics

The effect of temperature on the adsorption capacity of the polymer was determined in the range of 298–318 K. It was observed that adsorption was increased when the temperature increases as we obtained maximum sorption at 40 °C. After 40 °C, there was no significant change observed. The thermodynamic variables, i.e., enthalpy ($\Delta H°$), Gibbs free energy ($\Delta G°$) and entropy ($\Delta S°$) were also checked by using the following equation.
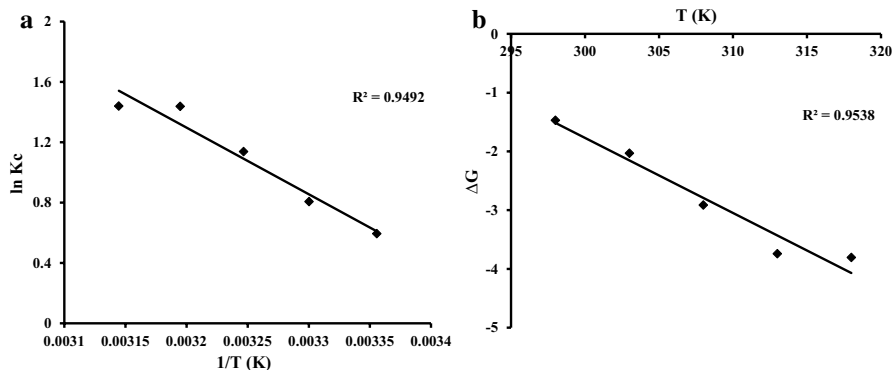
Fig. 10 **a** Van't Hoff plot, log *kc* versus 1/*T* and **b** effect of temperature on $\Delta G°$

Table 4 Different thermodynamic parameters for the sorption of As^{3+} on As-IP at different temperatures

Temperature (K)	$\Delta G°$ kJ/mol	$\Delta H°$ kJ/mol	$\Delta S°$	Correlation factor
298	− 1.470	36.7	0.128	0.953
303	− 2.032			
308	− 2.913			
313	− 3.741			
318	− 3.806			

$$\Delta G° = -RT \ln k$$

$$\ln k = -\Delta H°/RT + \Delta S°/R$$

$$\Delta S° = \Delta H° - \Delta G°/T$$

where $\Delta G°$ exhibits the Gibbs free energy (kJ/mol), *T* represents the temperature (K), *R* is the gas constant (0.008314 kJ/mol/K), K_c represents the equilibrium constant, $\Delta H°$ represents the enthalpy (kJ/mol) and $\Delta S°$ is entropy of the system (J/K).

The positive value of ΔH recommends that reaction was endothermic in nature. The positive value of $\Delta S°$ exhibits that randomness was increased during the sorption process and the negative value of $\Delta G°$ represents that reaction was spontaneous in nature (Fig. 10, Table 4).

Selectivity studies

To analyze the imprinting effect and ion recognition behavior of As-IP, the selectivity studies were used to carry out the presence of other competitive ions. This study was carried out by selecting Cr^{3+}, Al^{3+}, Ni^{2+}, Cu^{2+}, NO_3^-, PO_4^{3-} and SO_4^{2-} as other coexisting ions due to their size and properties. The result of K_d, K and K' of As^{3+} ions as compared to different other ions is listed in Table 5. K_d values of

Table 5 The selectivity studies of As^{3+} ion

Binary mixtures	Adsorbent	K_d As^{3+} (L/g)	K_d (M)	K	K'
As^{3+}/Cr^{3+}	As-IP	0.629	0.318	1.977	1.445
	NIP	0.271	0.198	1.368	
As^{3+}/Al^{3+}	As-IP	0.416	0.197	2.111	1.779
	NIP	0.108	0.091	1.186	
As^{3+}/Ni^{2+}	As-IP	0.743	0.364	2.041	1.469
	NIP	0.303	0.218	1.389	
As^{3+}/Cu^{2+}	As-IP	3.139	1.947	1.612	1.168
	NIP	1.281	0.928	1.380	
As^{3+}/NO^{3-}	As-IP	0.472	0.265	1.781	1.481
	NIP	0.184	0.153	1.202	
As^{3+}/PO_4^{3-}	As-IP	0.541	0.281	1.925	1. 802
	NIP	0.171	0.160	1.068	
As^{3+}/SO_4^{2-}	As-IP	0.627	0.242	2.590	2.367
	NIP	0.406	0.371	1.094	

As-IP for As^{3+} ions were higher than NIP, while the As-IP possess much greater K value than other coexisting ions. The K' values of As^{3+}/Cr^{3+}, As^{3+}/Al^{3+}, As^{3+}/Ni^{2+}, As^{3+}/Cu^{2+}, As^{3+}/NO^{3-}, As^{3+}/PO_4^{3-} and As^{3+}/SO_4^{2} were 1.445, 1.779, 1.469, 1.168, 1.481, 1.802 and 2.367, respectivley, which was more than 1. The results described that As-IP had high selectivity for As^{3+} ions in binary mixtures. As-IP has excellent selectivity toward As^{3+} ions as compared to other coexisting ions.

Reusability studies

Reusability study is a significant factor to use the adsorbent for practical usage. Reusability study of As-IP was carried out by using the adsorption–desorption method. The sorbed As^{3+} ions on As-IP were eliminated by using 15 mL of 1.0 M HCl. HCl was used as an active solvent to remove the As^{3+} ions from the polymeric matrix, and the percentage recovery was obtained up to 99.5%. The sorption–desorption cycle was checked up to ten times as shown in Fig. 11. After ten times, the recovery was decreased up to 1.93%. Thus, results showed that synthesized polymer has an excellent capability to remove the toxic As ions from aqueous media.

Comparison studies

The analytical features of synthesized As^{3+}-IIP were compared with reported adsorbent materials for the sorption of As^{3+} ion on the basis of sorption capacity, polymerization technique and sample source as shown in Table 6. The maximum sorption capability was obtained using 10 mg/L concentration. It can be observed that As^{3+}-IIP holds excellent sorption capacity and good selectivity for As^{3+} ion.
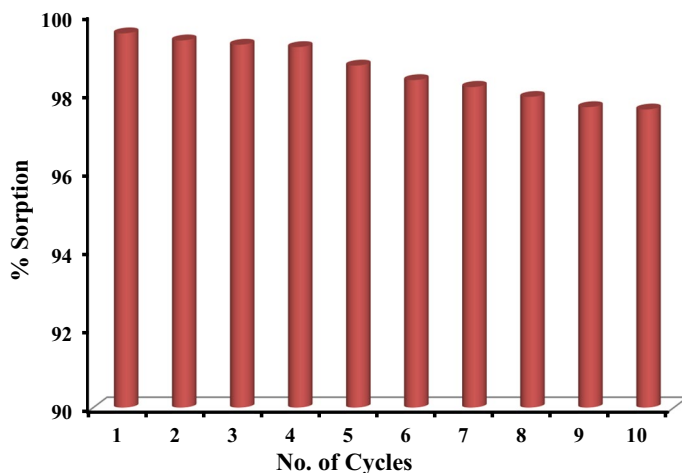
Fig. 11 Reusability studies of As-IP

Table 6 Comparison As-IIPs with previously reported studies

Polymerization technique	Adsorption material	Adsorption Capacity (mg/g)	Sample source	References
Microwave-assisted precipitation polymerization	As^{3+}-IP	0.1750	Water sample	[6]
Precipitation polymerization	As^{3+}-IP	–	Water sample	[35]
Precipitation polymerization	Polymer composite adsorbents	20.62	Water sample	[34]
Graft polymerization	Arsenate anion IPs	0.17	Water sample	[36]
Graft polymerization	As(III)-imprinted chitosan resin	4.16	Juice	[37]
Bulk polymerization	Tailoring ion-imprinted polymer	0.0905	Water	[38]
Precipitation polymerization	As^{3+}-IPs	106.3	Wastewater	This work

Consequently, results indicated that prepared novel As^{3+}-IIP was highly selective sorbent for detoxification of As^{3+} ion from aqueous system.

Real water samples

The analytical application of As-IP was carried out as an efficient adsorbent for the removal of toxic As ions under optimal conditions. The excellent linearity range was achieved in the concentration range of 10–100 µg/L. The limit of detection (LOD) (3SD/m) and limit of quantification (LOQ) (10SD/m) were achieved as 0.87 µg/L and 2.9 µg/L, respectively, where SD represents the standard deviation and m is the slope of the calibration graph. The LOD and LOQ values were

Table 7 Analytical features of the prepared extraction and pre-concentration method

Range	10–100 (µg/L)
R^2	0.993
%RSD ($n = 10$)	4.2
LOD	0.87
LOQ	2.9

Table 8 Spiked recovery test of As^{3+} in real water samples of channel canal Hyderabad

Sample	S1	S2	S3	S4	S5
Without addition	12.7 ± 0.36	11.4 ± 0.29	14.59 ± 0.68	16.8 ± 0.4	13.1 ± 0.52
As^{3+} added	20	20	20	20	20
As^{3+} found	$32.1.3 \pm 0.52$	30.9 ± 0.47	33.9 ± 0.35	36.44 ± 0.59	$32.87.3 \pm 0.29$
% recovery	97	97.5	96.5	98.2	98.8

satisfactory for the selective elimination of As^{3+} from aqueous media. The values of LOD, LOQ and R^2 and linear concentration are given in Table 7. To achieve more accurate results, the synthesized adsorbent was applied on real water samples for the trace elimination of As^{3+} ions. For this purpose, several experiments were done on water samples by using the standard addition method by spiking of 20 µg/L in each sample and results are shown in Table 8.

Conclusion

In this work, we report the preparation of As-IP by using precipitation polymerization, 4-VP, 2-HEMA as ligand and functional monomer, EGDMA as a crosslinker and AIBN as an initiator in the methanol solvent. The EDX and FT-IR results shows that the As^{3+} is completely imprinted on the polymer matrix. The irregular shape and high porosity of As-IP were carried out by using SEM. Different parameters optimized to find maximum sorption efficiency, i.e., pH, agitation time, sorbent dose and shaking speed. The sorption of IIPs is rapid and followed the Langmuir isotherm model and pseudo-second-order kinetic model. The maximum sorption capacity found 106.3 mg/g (initial concentration of metal ion 5 mg/L) at the pH 6.0. The relative selective coefficient of all As^{3+}/coexisting ions is more than one due to the existence of specific binding sites of As^{3+} in a polymer matrix. Therefore, the new synthetic IPs are highly selective for the selective sorption of As^{3+} ions from an aqueous media at trace level.

References

1. dos Santos Costa BE, Coelho NMM, Coelho LM (2015) Determination of arsenic species in rice samples using CPE and ETAAS. Food Chem 178:89–95
2. Fang L, Min X, Kang R, Yu H, Pavlostathis SG, Luo X (2018) Development of an anion imprinted polymer for high and selective removal of arsenite from wastewater. Sci Total Environ 639:110–117
3. Bang S, Patel M, Lippincott L, Meng X (2005) Removal of arsenic from groundwater by granular titanium dioxide adsorbent. Chemosphere 60:389–397
4. Li R, Li Q, Gao S, Shang JK (2012) Exceptional arsenic adsorption performance of hydrous cerium oxide nanoparticles: part A. Adsorption capacity and mechanism. Chem Eng J 185:127–135
5. Brahman KD, Kazi TG, Afridi HI, Baig JA, Arain SS, Talpur FN, Kazi AG, Ali J, Panhwar AH, Arain MB (2016) Exposure of children to arsenic in drinking water in the Tharparkar region of Sindh, Pakistan. Sci Total Environ 544:653–660
6. Mustafai FA, Balouch A, Jalbani N, Bhanger MI, Jagirani MS, Kumar A, Tunio A (2018) Microwave-assisted synthesis of imprinted polymer for selective removal of arsenic from drinking water by applying Taguchi statistical method. Eur Polym J 109:133–142
7. Shah AQ, Kazi TG, Arain MB, Jamali MK, Afridi HI, Jalbani N, Baig JA, Kandhro GA (2009) Accumulation of arsenic in different fresh water fish species–potential contribution to high arsenic intakes. Food Chem 112:520–524
8. Lata S, Samadder S (2016) Removal of arsenic from water using nano adsorbents and challenges: a review. J Environ Manag 166:387–406
9. Thakur S, Govender PP, Mamo MA, Tamulevicius S, Mishra YK, Thakur VK (2017) Progress in lignin hydrogels and nanocomposites for water purification: future perspectives. Vacuum 146:342–355
10. Cheng W, Ding C, Wang X, Wu Z, Sun Y, Yu S, Hayat T, Wang X (2016) Competitive sorption of As (V) and Cr(VI) on carbonaceous nanofibers. Chem Eng J 293:311–318
11. Song W, Wang X, Chen Z, Sheng G, Hayat T, Wang X, Sun Y (2018) Enhanced immobilization of U (VI) on Mucor circinelloides in presence of As (V): batch and XAFS investigation. Environ Pollut 237:228–236
12. Kumar A, Balouch A, Pathan AA, Mahar AM, Abdullah MS, Jagirani FA, Mustafai M, Zubair B Laghari, Panah P (2017) Remediation techniques applied for aqueous system contaminated by toxic Chromium and Nickel ion. Geol Ecol Landsc 1:143–153
13. Balouch A, Jagirani MS, Mustafai FA, Tunio A, Sabir S, Mahar AM, Rajar K, Shah MT, Samoon MK (2017) Arsenic remediation by synthetic and natural adsorbents. Pak J Anal Environ Chem 18:18–36
14. Yang X, Xia L, Song S (2017) Arsenic adsorption from water using graphene-based materials as adsorbents: a critical review. Surf Rev Lett 24:1730001
15. Thakur S, Sharma B, Verma A, Chaudhary J, Tamulevicius S, Thakur VK (2018) Recent approaches in guar gum hydrogel synthesis for water purification. Int J Polym Anal Charact 23:621–632
16. Kumar A, Balouch A, Pathan AA, Jagirani MS, Mahar AM, Zubair M, Laghari B (2019) Remediation of Nickel ion from wastewater by applying various techniques: a review. Acta Chem Malays 3:1–5
17. Sert S, Celik A, Tirtom VN (2017) Removal of arsenic (III) ions from aqueous solutions by modified hazelnut shell. Desalin Water Treat 75:115–123
18. Rathore VK, Dohare DK, Mondal P (2016) Competitive adsorption between arsenic and fluoride from binary mixture on chemically treated laterite. J Environ Chem Eng 4:2417–2430
19. Thakur S, Chaudhary J, Kumar V, Thakur VK (2019) Progress in pectin based hydrogels for water purification: trends and challenges. J Environ Manag 238:210–223
20. Thakur S, Govender PP, Mamo MA, Tamulevicius S, Thakur VK (2017) Recent progress in gelatin hydrogel nanocomposites for water purification and beyond. Vacuum 146:396–408
21. Thakur S, Sharma B, Verma A, Chaudhary J, Tamulevicius S, Thakur VK (2018) Recent progress in sodium alginate based sustainable hydrogels for environmental applications. J Clean Prod 198:143–159
22. Chen L, Wang X, Lu W, Wu X, Li J (2016) Molecular imprinting: perspectives and applications. Chem Soc Rev 45:2137–2211

23. Roushani M, Abbasi S, Khani H (2015) Synthesis and application of ion-imprinted polymer nano-particles for the extraction and preconcentration of copper ions in environmental water samples. Environ Monit Assess 187:219
24. Fu J, Chen L, Li J, Zhang Z (2015) Current status and challenges of ion imprinting. J Mater Chem A 3:13598–13627
25. Meouche W, Laatikainen K, Margaillan A, Silvonen T, Siren H, Sainio T, Beurroies I, Denoyel R, Branger C (2017) Effect of porogen solvent on the properties of nickel ion imprinted polymer materials prepared by inverse suspension polymerization. Eur Polym J 87:124–135
26. Lenoble V, Laatikainen K, Garnier C, Angeletti B, Coulomb B, Sainio T, Branger C (2016) Nickel retention by an ion-imprinted polymer: wide-range selectivity study and modelling of the binding structures. Chem Eng J 304:20–28
27. Fang L, Xiao X, Kang R, Ren Z, Yu H, Pavlostathis SG, Luo J, Luo X (2018) Highly selective adsorption of antimonite by novel imprinted polymer with microdomain confinement effect. J Chem Eng Data 63:1513–1523
28. Zhao H, Ye Y, Cao S, Dai J, Li L (2014) Synthesis and properties of cadmium (II)-imprinted polymer supported by magnetic multi-walled carbon nanotubes. Anal Methods 6:9313–9320
29. Kumar A, Balouch A, Pathan AA, Abdullah, Jagirani MS, Mahar AM, Rajput M-U-H (2019) Novel chromium imprinted polymer: synthesis, characterization and analytical applicability for the selective remediation of Cr(VI) from an aqueous system. Int J Environ Anal Chem 99:454–473
30. Balouch A, Talpur FN, Kumar A, Shah MT, Mahar AM (2019) Synthesis of ultrasonic-assisted lead ion imprinted polymer as a selective sorbent for the removal of Pb^{2+} in a real water sample. Microchem J 146:1160–1168
31. Li H, Li J, Cheng L (2015) Novel Cr(III) surface magnetic ion-imprinted materials based on graphene oxide for selective removal of Cr(III) in aqueous solution. Desalination Water Treat 56:204–215
32. Kumar A, Balouch A, Pathan AA (2019) Synthesis, adsorption and analytical applicability of Ni-imprinted polymer for selective adsorption of Ni^{2+} ions from the aqueous environment. Polym Test 77:105871
33. Zhou Z, Kong D, Zhu H, Wang N, Wang Z, Wang Q, Liu W, Li Q, Zhang W, Ren Z (2018) Preparation and adsorption characteristics of an ion-imprinted polymer for fast removal of Ni (II) ions from aqueous solution. J Hazard Mater 341:355–364
34. Önnby L, Pakade V, Mattiasson B, Kirsebom H (2012) Polymer composite adsorbents using particles of molecularly imprinted polymers or aluminium oxide nanoparticles for treatment of arsenic contaminated waters. Water Res 46:4111–4120
35. Alizadeh T, Rashedi M (2014) Synthesis of nano-sized arsenic-imprinted polymer and its use as As^{3+} selective ionophore in a potentiometric membrane electrode: part 1. Anal Chim Acta 843:7–17
36. Gao B, Du J, Zhang Y (2013) Preparation of arsenate anion surface-imprinted material IIP-PDMC/SiO2 and study on its ion recognition property. Ind Eng Chem Res 52:7651–7659
37. Liu B, Wang D, Gao X, Zhang L, Xu Y, Li Y (2011) Removal of arsenic from *Laminaria japonica Aresch* juice using As (III)-imprinted chitosan resin. Eur Food Res Technol 232:911
38. Tsoi Y-K, Ho Y-M, Leung KS-Y (2012) Selective recognition of arsenic by tailoring ion-imprinted polymer for ICP-MS quantification. Talanta 89:162–168